

## Detailed Survey of Dust Particles from JET with the ITER Like Wall: Origin, Composition and Internal Structure

E. Fortuna-Zaleśna<sup>1\*</sup>, J. Grzonka<sup>1,2</sup>, M. Rubel<sup>3</sup>, A. Widdowson<sup>4</sup>, A. Garcia-Carrasco<sup>3</sup>,  
P. Petersson<sup>3</sup>, A. Baron-Wiecheć<sup>4</sup> and JET Contributors<sup>4,\*\*</sup>

<sup>1</sup>Department of Materials Science, Warsaw University of Technology, 01-152 Warsaw, Poland

<sup>2</sup>Institute of Electronic Materials Technology, 133 Wolczynska Str., 01-919 Warsaw, Poland

<sup>3</sup>Fusion Plasma Physics, Royal Institute of Technology (KTH), SE-10044 Stockholm, Sweden

<sup>4</sup>EUROfusion Consortium, JET, Culham Science Centre, Abingdon, OX14 3DB, UK

\*\* See the author list of “Overview of the JET results in support to ITER” by X. Litaudon et al. to be published in Nuclear Fusion Special issue: overview and summary reports from the 26th Fusion Energy Conference (Kyoto, Japan, 17-22 October 2016)

*E-mail contact of main author: efortuna@inmat.pw.edu.pl*

**Abstract.** Results are presented for the dust survey performed at JET after the second experimental campaign with the ITER-Like Wall: 2013-2014. Samples were collected on adhesive stickers from several different positions in the divertor both on the tiles and on the divertor carrier. Comprehensive characterization accomplished by a wide range of high-resolution microscopy techniques, including focused ion beam, has led to the identification of several classes of particles: (i) beryllium flakes originating either from the Be coatings from the inner wall cladding or Be-rich mixed co-deposits resulting from material migration; (ii) beryllium droplets and splashes; (iii) tungsten and nickel-rich (from Inconel) droplets; (iv) mixed material layers with a various content of small (8 - 200 nm) W-Mo and Ni-based debris. A significant content of nitrogen from plasma edge cooling has been identified in all types of co-deposits. A comparison between particles collected after the first and second experimental campaign is also presented and discussed.

### 1. Introduction

Comprehensive and systematic surveys of dust particles generated in tokamaks have been carried out in order to provide data needed in the licensing process of ITER. In this sense, surveys of dust and co-deposits in JET with the ITER-Like Wall (JET-ILW) are the most relevant for next-step devices with metal walls. It should be stressed that the amount of loose dust removed by vacuum cleaning of the divertor after two experimental campaigns (2011-2012 and 2013-2014) was around 1 g after each operation period, i.e. over two orders of magnitude less [1-3] than after the operation of JET with carbon walls. Even though the quantities in JET-ILW are small, the study of dust particles is crucial for ITER, because these are unique data from a full metal-wall (beryllium and tungsten) machine. The identification of various categories of particles allows conclusions on mechanisms underlying their generation and mobilisation.

### 2. Experimental

The study was carried out for samples collected on tiles from the divertor modules which were not vacuum cleaned after the 2013-2014 campaign. Two complete modules equipped with erosion-deposition diagnostics [4] were transferred from the torus to the Beryllium Handling Facility (BeHF). Dust sampling was done manually at several different positions

using adhesive carbon pads of 2.54 cm (1 inch) in diameter. This method enables a direct correlation between the location and the type of dust particles. However, the procedure has one disadvantage: only the bottom part and some side surfaces of the collected matter can be examined by optical or scanning electron microscopy (SEM), because the top layer is embedded in the glue of a pad. This problem is partly overcome by using focused ion beam (FIB) technique to obtain cross-sections of particles, but even this approach still prevents direct studies of the top layers. It is also limited to objects not thicker than 20 micrometers; above that value the quality of results is degraded. The information on the sampling is detailed in Table 1, while images in Figure 1 show the divertor poloidal cross-section.

TABLE I. LIST OF STUDIED MATERIALS WITH DETAILS ON THEIR ORIGIN AND SAMPLING LOCATION.

Tile / sample	Region	S-coordinate (mm)
0 (35)	Outside deposition zone	50
0 (31)	Deposition zone	137
1(24)	Apron (horizontal part of Tile 1)	210
3 (1)	Lower part below	590
6 (11)	Deposition zone in shadow of Tile 7	1415
Under Tile 6	Divertor carrier	n/a

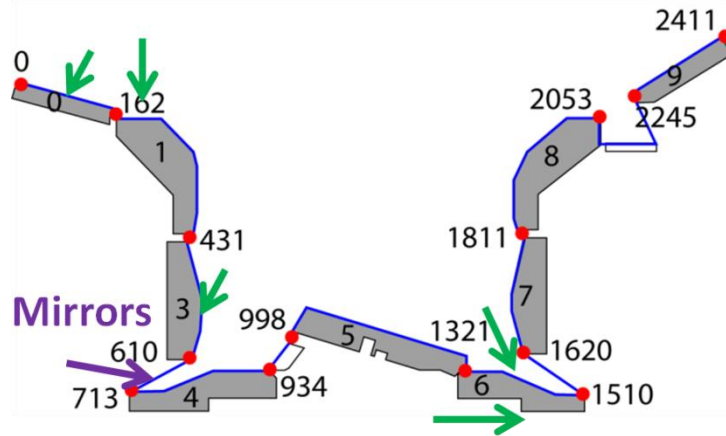


FIG. 1. Divertor cross-section in JET-ILW.

Dust found under Tile 6 on the frame of the divertor carrier was collected by wiping with a swab and then the matter was transferred to a sticky pad.

The composition, size, surface topography and internal features of dust and deposits were examined using a large set of electron and ion beam methods. The analyses performed at the Warsaw University of Technology comprised: SEM (Hitachi SU 8000) combined with energy-dispersive X-ray spectroscopy (EDX, Thermo Scientific Ultra Dry, type SDD enabling Be analysis), focused ion beam (FIB/SEM, Hitachi NB5000) and scanning transmission electron microscopy (STEM, Aberration Corrected Dedicated STEM Hitachi HD-2700). Depth profiling (Be, C, N, O, W) was determined by time-of-flight heavy ion elastic recoil detection analysis (ToF-ERDA) with a 36 MeV  $^{127}\text{I}^{8+}$  beam. The method gives good depth resolution of a few nm and it is particularly suited for studying smooth surfaces, e.g. mirrors. The information depth is limited to a few hundreds of micrometers because of a low incidence angle ( $22^\circ$ ). Global fuel retention studies (i.e. deuterium content analysis) could not be performed on samples collected by sticky pads. Thermal desorption, for obvious reasons, is out of question.

### 3. Results and discussion

The presentation of dust survey follows the divertor poloidal cross-section starting from the inner divertor Tile 0 which acts as the High Field Gap Closure (HFGC) plate. A comparison of dust after the consecutive campaigns will be made for apron on Tile 1. The description of dust collected from plasma-facing surfaces will be complemented by the characterisation of particles taken from the divertor carrier below Tile 6.

#### *Dust on divertor tiles*

Tile 0 has two distinct regions which can be perceived in Fig. 1(b). A sample collected outside the “blackish” deposition zone is characterised by a small density of particles: thin though fairly large (up to 300  $\mu\text{m}$ ) flakes rich in beryllium. It is documented by the image of a flakes in Fig. 2(a). The corresponding X-ray spectrum, Fig 2(b) clearly proves that Be is the major constituent. The structure of the flakes has features of Be coatings from the inner wall cladding tiles, as observed in secondary electron images. The structure of some areas suggests that the material was molten.

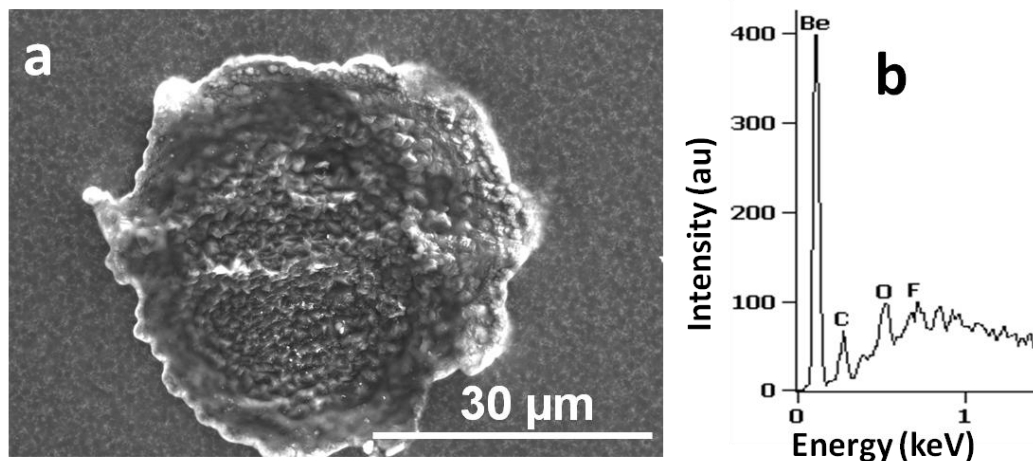


FIG. 2. (a) Beryllium flakes from the inner wall cladding on Tile 0 in the area without deposits and (b) corresponding EDX spectrum.

Images in Fig. 3 show particles of mixed columnar and stratified structure detached from the deposition zone: thick and cracked Be-based layers. There are regions rich in tungsten and nickel: bright areas in Fig. 3(b) recorded in the backscattered electron (BSE) mode and analysed with EDX. While the presence of tungsten may be attributed to the detachment of underlying W coating on the CFC tile, the presence of nickel can only be related to the deposition of that element eroded from the in-vessel Inconel components: torus wall or a grill of the antenna for ion or electron resonance heating, or from damaged tie rods in Tile 7. The studied region on Tile 0 is known to be the major deposition zone in the divertor with the deposit thickness reaching 50  $\mu\text{m}$  (cumulative after two campaigns) and the deuterium content of up to  $1 \times 10^{19} \text{ cm}^{-2}$ .

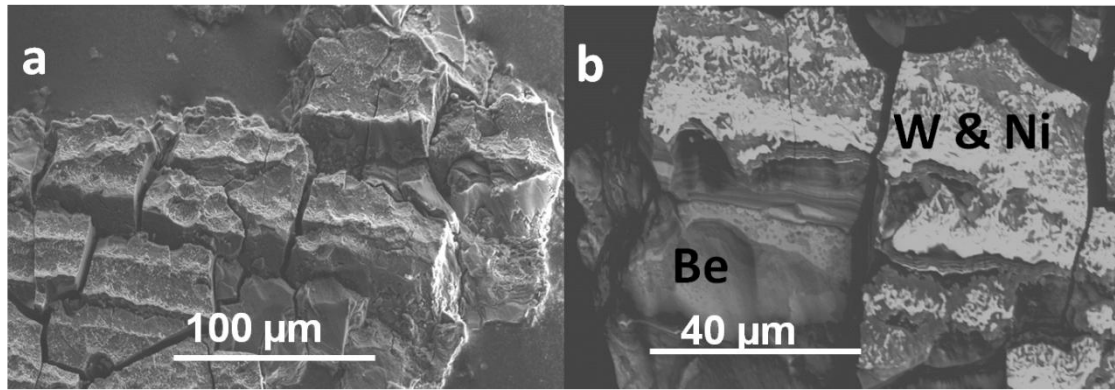


FIG. 3. Thick co-deposits collected in the deposition zone of Tile 0 after ILW-2.

For Tile 1 the analyses have been concentrated on the apron area which may be perceived as the extension of Tile 0, also from the point of view of deposition: layers up to 20  $\mu\text{m}$  thick [5-7]. Dust from the apron was sampled after each campaign. This allows for a meaningful comparison because the operation time was similar in both cases: around 19.5 h including approximately 6.5 h of limiter and 13 h of X-point plasmas. After the first campaign the most important result was the identification of Be dust in the form of droplets and flakes detached from co-deposited layers. The internal structure of such flakes has been recently examined. STEM images in Fig. 4(a) and (b) show, respectively, the bottom and top layer of a 4  $\mu\text{m}$  thick flake formed during ILW-1. Bottom of the layer corresponds to the initial phase of operation, while the top is related to end of the 2011-2012 ILW campaign. A crystalline columnar structure suggests quiescent growth of the deposit. The layer contains also tiny tungsten particles: very small amount at the beginning, Fig 4(a). Significantly increased deposition of 8-15 nm W particles occurred at the final stages of operation; it is shown in Fig. 4(b). The presence of W inclusions is most probably attributed to the erosion of W-coated carbon fibre composite (W/CFC) tiles in the divertor and some places on the main chamber wall. As a consequence, the composition of deposits is clearly correlated with the history of operation: L-mode in the initial phase and a greater input power for H-mode discharges towards the end. Disruptions at high power shots additionally contributed to the generation of tiny metal particles.

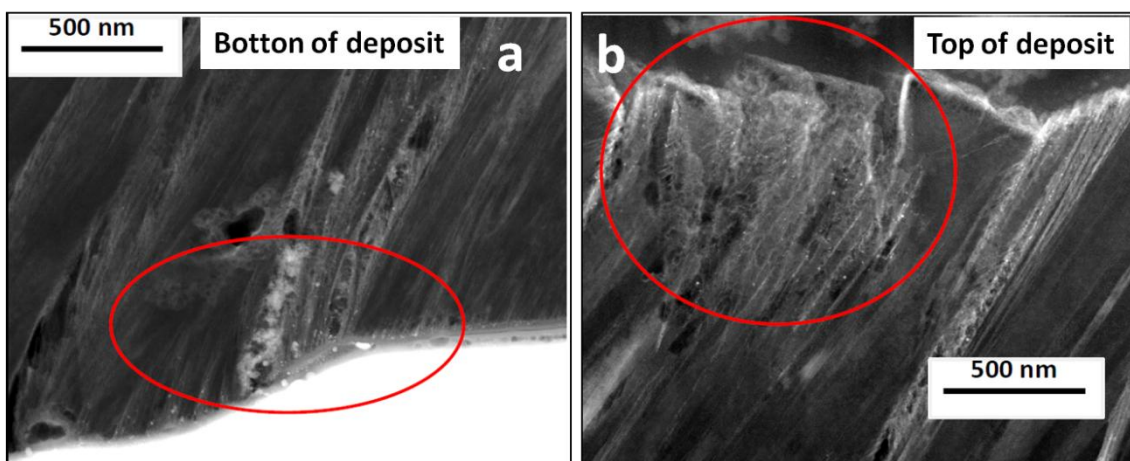
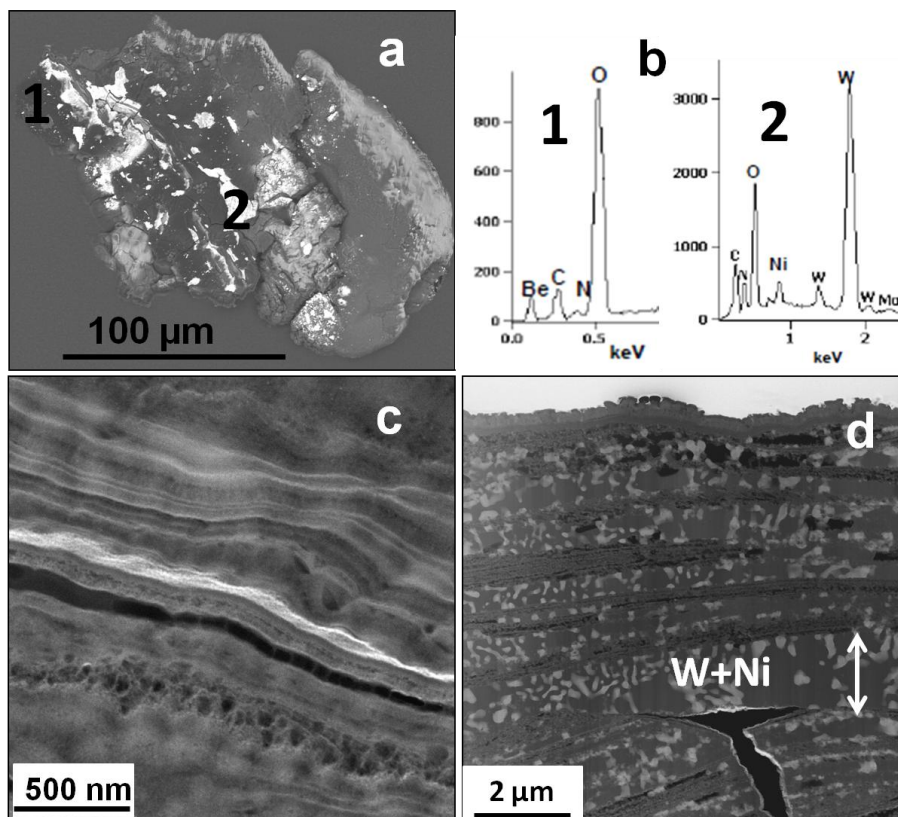


FIG. 4. STEM images of: (a) the bottom and (b) top layer of beryllium flake on apron of Tile 1 after the ILW-1 campaign in 2011-2012.

Examples of dust collected from the Tile 1 apron after the second campaign with most discharges in the H-mode are in Fig. 5 (a)-(d), showing a 200  $\mu\text{m}$  object, EDX spectra from two regions (marked 1 and 2) and STEM images for cross-sections from two different areas of that object. Already an overview BSE image in Fig. 5(a) indicates a complex mix of light and heavy elements. A cross section in Fig. 5(c) recorded in the high-angle-annular dark field (HAADF) mode shows fairly uniform co-deposit composed of low-Z elements (Be, C, O, N) with only one remarkable tungsten layer visible as a bright stripe. Another cross-section, Fig. 5(d), is a sandwich of low-Z (beryllium-carbon) strata and regions with 100-200 nm inclusions of heavy metals (tungsten and nickel) in the low-Z matrix. Tungsten can originate both from the bulk metal (Tile 5) and coated tiles, but nickel must come from Inconel or steel components. There are no such Ni-rich parts in the vicinity of Tile 1. One may suggest that the particle was formed in another location (e.g. Tile 6 where Ni droplets appeared because of damaged Inconel tie rods of Tile 7) and then it was mobilised by a disruption. This statement is justified by the fact that two cross-sections described above are only 100  $\mu\text{m}$  apart. Therefore, such big differences in morphology cannot be attributed to not uniform deposition. A big particle is not a regular flake but an agglomerate of small particulates formed originally on the apron and in other places. It should be stressed that all types of co-deposits after the 2013-2014 campaign (dominated either by light or heavy elements) contain significant amounts of nitrogen retained after plasma edge cooling by gas injection. Nitrogen retention in JET co-deposits has already been reported [6,8], but the dust studies show that nitrogen is present in all types of re-deposited materials. Corresponding X-ray spectra deposit are in Fig. 5(b).



*FIG. 5. Deposits on apron of Tile 1 after ILW-2 campaign in 2013-2014: (a) a typical agglomerated particle, (b) EDX spectra from two regions, (c) stratified Be-rich deposit; (d) highly porous mixed deposit with light and heavy elements.*

Rounded beryllium objects, 8-10  $\mu\text{m}$  in diameter and smaller, have been detected on the apron. A small spherical Be droplet shown in Fig. 6 originates most probably from a melt layer on overheated limiters. The volume of a sphere of 10  $\mu\text{m}$  in diameter is  $5.25 \times 10^{-10} \text{ cm}^3$ , what corresponds to less than 1 ng in weight and  $6.5 \times 10^{13}$  atoms, at atomic density of  $1.24 \times 10^{23} \text{ cm}^{-3}$ . In a single sphere there is only a tiny amount of matter. However, from ex-situ analyses it is not possible to conclude on the amount of material ablated when the droplet was passing plasma from the place of origin. Based on the photographic survey, events of limiter melting related to disruptions were not unique and some of them could cause certain material losses.

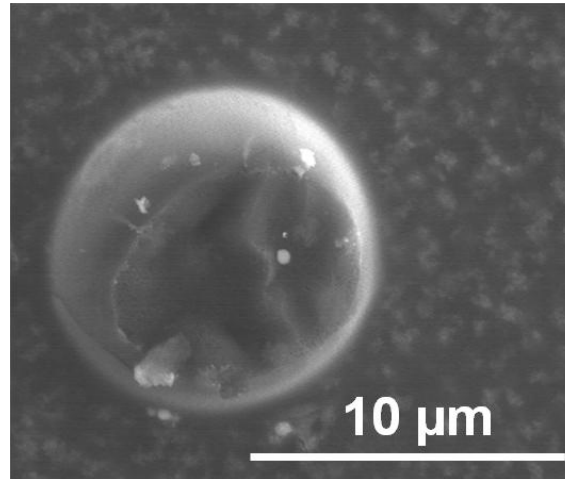


*FIG. 6. A spherical beryllium particle on apron of Tile 1 after the first ILW campaign.*

Matter collected from Tile 3 contains only small carbon-based and ceramic particles. Fairly clean and dust-free tile surfaces could be expected given the fact that the strike point was on that tile during majority of pulses in 2013-2014.

A sloping part of Tile 6 is a deposition zone and this is reflected by character of particles which are similar to what has been detected in the deposition zone of Tile 0 and on the apron of Tile 1, i.e. these are mainly fragments of co-deposits. The detached flakes are relatively large – up to 200  $\mu\text{m}$  in size. They have a layered structure, although granular forms are detected as well. Both composition and internal structure are diversified. The regions rich in either light (Be, C, N, O) and or heavy elements are present (W or/and Ni). Although a distinct Be peak was visible only in one spectrum, a high oxygen peak registered in other EDX spectra taken from the areas rich in light elements indicates that Be is a major constituent of these particles.

Particles/layers rich in tungsten (originating from the W coating) and nickel are detected at the bottom part of particles being small fragments of co-deposit. They have different forms: the smallest objects observed with SEM are fine nanoparticles embedded in the matrix composed of light elements (Fig. 7) whereas the largest observed pieces are several microns in size.

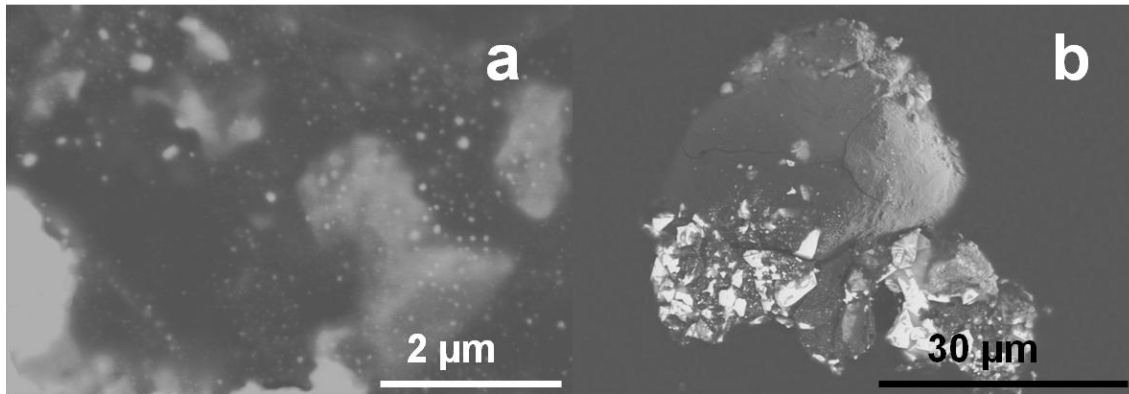


FIG. 7. Particles rich in tungsten present in deposits originating from Tile 6, BSE mode.

#### *Dust on the divertor carrier*

Two main groups of particles have been found on the sample collected by brushing the divertor carrier under Tile 6: (i) detached fragments of W-Mo coatings and (ii) beryllium-rich flakes. The size of W or W-Mo debris ranges from several hundred of  $\mu\text{m}$  to a few mm. Their surface was overheated, locally revealing melt zones. The largest Be-rich particle was approximately 2x2 mm in size. Its general appearance and internal structure are presented in Figures 8(a) and (b), respectively. The surface is uniform: morphology and elemental composition are changed within the individual flake limits. The deposit is composed of fine particles/grains, Fig. 8(b), thus making the structure very porous. This form of beryllium deposit has been observed for the first time. Other particles composed of different constituents have been also detected: carbon, ceramics and metals, namely steel, Inconel and copper.

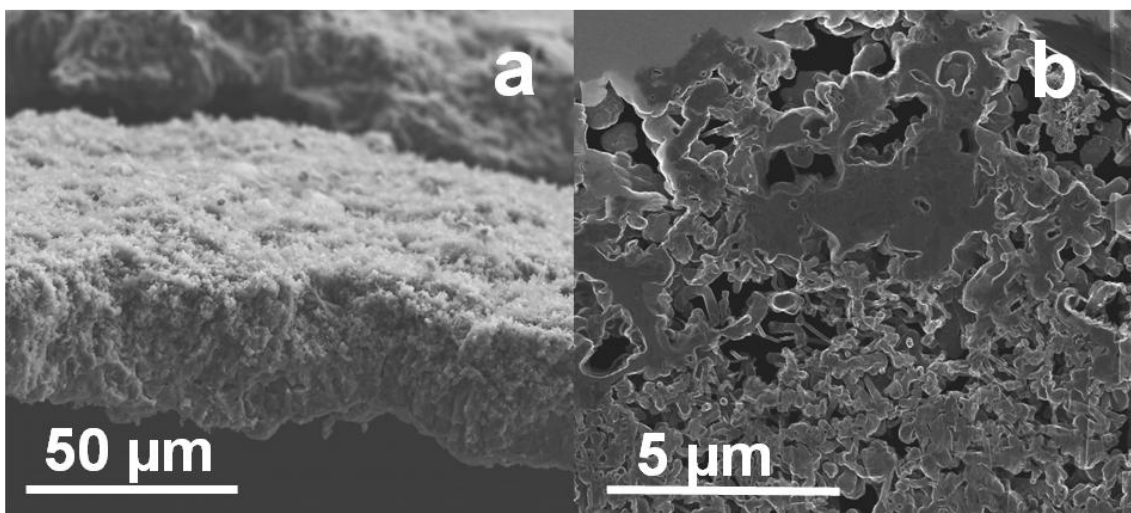


FIG. 8. Be-rich co-deposit on the divertor carrier under Tile 6 after ILW-2: a) SEM image of fractured edge, b) STEM image of internal structure.

#### **4. Concluding remarks**

The most important result of dust surveys is the small amount of loose matter (1.5 g level) retrieved after ILW campaigns. Examination of dust sampled from various regions of the divertor has identified a range of particles. Besides not ITER-relevant debris from tungsten

coatings on CFC tiles there are two major classes of importance to ITER: (i) mixed deposits rich in beryllium and (ii) metal droplets (Be, W, Ni) born in melting events of wall materials. Further split into sub-categories is not intended here for a single reason: the comparison of deposits from the two campaigns clearly proves the increased complexity of particles due to agglomeration of particles formed originally under different conditions and, most probably, in different places. This indicates mobilisation and transport of fine dust, for instance, as a consequence of off-normal events. Therefore, conclusions regarding the size range should be rather restricted to metal droplets and splashes (from 3  $\mu\text{m}$  for droplets to 100  $\mu\text{m}$  for splashes), but certainly not to agglomerates or even co-deposits, which are brittle and easily disintegrate into smaller objects.

In summary, tile analyses and locally-specific dust survey provide very detailed data on the overall morphology of particles. High-resolution dust studies allow, to fair extent, for conclusions on dust generation, its migration and agglomeration. An important contribution of this work to PWI studies in a metal-wall tokamak is a detailed insight into properties of deposits formed on diagnostic components, i.e. mirrors. Transport of light (Be) and heavy (W) metals to the shadowed region in the divertor is well documented once again [8] and it is also shown that such metal layers brake and form dust.

### Acknowledgement

This work has been carried out within the framework of the EUROfusion Consortium and has received funding from the Euratom research and training programme 2014-2018 under grant agreement No 633053. The views and opinions expressed herein do not necessarily reflect those of the European Commission.

### References

- [1] WIDDOWSON A. et al., “Material migration patterns and overview of first surface analysis of the JET ITER-like wall”, Phys. Scr. T159 (2014) 014010
- [2] WIDDOWSON A. et al. This Conference
- [3] BARON-WIECHEC A. et al., “First dust study in JET with the ITER-like wall: sampling, analysis and classification”, Nucl. Fusion 55 (2015) 113033.
- [4] RUBEL M. et al., “Overview of erosion–deposition diagnostic tools for the ITER-Like Wall in the JET tokamak”, J. Nucl. Mater. 438 (2013) S1204.
- [5] LIKONEN J. et al., “First results and surface analysis strategy for plasma-facing components after JET operation with the ITER-like wall”, Phys. Scr. T159 (2014) 014016.
- [6] PETTERSSON P. et al., “Co-deposited layers in the divertor region of JET-ILW”, J. Nucl. Mater. 463 (2015) 814.
- [7] MAYER M. et al., “Erosion and deposition in the JET divertor during the first ILW campaign”, Phys. Scr. T167 (2016) 014051.
- [8] IVANOVA D. et al., “An overview of the comprehensive First Mirror Test in JET with ITER-like wall”, Phys. Scr. T159 (2014) 014011.